RILEM Technical Letters (2022) 7: 88-97
https://doi.org/10.21809/rilemtechlett.2022.164

Estimating Na^+ and K^+ concentrations of the pore solution based on ex-situ leaching tests and thermodynamic modeling

Atolo Tuinukuafe[1], Krishna Siva Teja Chopperla[1], W. Jason Weiss[1], Jason H. Ideker[1], O. Burkan Isgor[1,*]

[1] School of Civil and Construction Engineering, Oregon State University, Corvallis, OR, USA

Received: 11 June 2022 / Accepted: 14 September 2022 / Published online: 14 October 2022

Abstract

Ex-situ leaching (ESL) methods have typically yielded higher sodium and potassium concentrations than pore solutions obtained using the conventional high-pressure extraction approach since ESL concentrations require a back-calculation to account for dilution. This paper proposes a new method for adjusting the concentrations obtained from ESL. Thermodynamic calculations were used to determine the total pore solution content, and a pore partitioning model was then used to separate the total solution into gel and capillary assignments. Using the refined pore solution volumes to adjust the concentrations from ESL improved the correlation to PSE concentrations.

Keywords: Cement; Pore Solution; Leaching; Thermodynamic Modeling

1 Introduction

The alkali content of the pore solution of hardened concrete has a strong effect on the long-term performance and durability of concrete structures. Alkalis in the pore solution keep the pH of concrete high which helps maintain the passivity of embedded steel reinforcement [1]. They also affect the resistivity of the pore solution [2], which is a critical parameter in the kinetics of reinforcement corrosion in concrete after the loss of passivity due to chloride ingress or carbonation [3,4]. The resistivity of pore solution is also needed in the calculation of the formation factor of concrete, which is used to calculate the transport properties of concrete [5,6]. Alkali ions in the pore solution may also lead to deleterious alkali-aggregate reactions when reactive aggregate is present [7-9]. Therefore, accurate quantification of alkali content of concrete pore solution is critical; however, this is not always an easy task.

High-pressure pore solution extraction (PSE) performed on a hardened cement paste, mortar, or concrete sample is a widely-used technique for pore solution analysis as it expresses the liquid directly from the crushed sample [10-15]. However, the feasibility of PSE is affected by the binder type, water-to-binder ratio (w/b), and aggregates – when present – since sufficient available pore water is required for expression. Sample preparation and conditioning prior to PSE could also influence results [13]. Ex-situ leaching (ESL) methods are a potential alternative that can be readily applied to any sample – regardless of moisture content, age, carbonation status, or w/b [11].

ESL test methods typically begin by pulverizing the sample to increase its surface area and remove as many coarse aggregate particles as possible in the case of concrete. During this process water may be lost from the system due to evaporation making it difficult to know the initial water content of the powder, which is a potential source of error that will be discussed later [11]. The second step of ESL methods generally involves stirring the powdered sample in a solvent, which is most commonly deionized water, and then filtering to obtain a diluted solution for chemical analysis. Several studies on ESL test methods have investigated in numerous factors, including the temperature of the leaching solution [10,16] (Natkunarajah et al. recently showed a negligible effect of solution temperature on the results of ESL for concrete [24]), liquid-to-solid ratio [16-20], the duration of the leaching period [19,21,22], and the particle size of the pulverized sample [16,19,21,22]. The list of ex-situ leaching methods resulting from multiple studies includes cold water extraction (CWE) [9,18,19,21–24], hot water extraction (HWE) [13,25], and the "espresso" method [11,26]. These methods have been used to obtain the alkali metal content in g/g of dry sample – a useful metric for AAR studies [9].

Despite advancements in ESL methods, the accuracy of the ESL results with respect to PSE is unclear, and there are examples of ESL methods yielding pore solution concentrations of Na^+ and K^+ (generally referred to as the alkali concentration in cement literature) that are significantly higher than the PSE method. For example, Berube and Tremblay observed higher sodium concentrations from HWE compared to PSE [13]. The ESL methods investigated by

*Corresponding author: O. Burkan Isgor, burkan.isgor@oregonstate.edu

Plusquellec et al. included the CWE method and showed higher alkali contents than PSE [11]. The method of determining of free water content for correcting ESL concentrations has been identified as a potential source of error by multiple authors [11,24].

Because water is added to the sample during ESL methods, the concentration of ions (i.e., concentration assumed to be assessed by PSE) must account for the water added. This is done using Eq. 1:

$$C_{PSE} = C_{ESL}\frac{V_{ESL}}{V_{PSE}} \quad (1)$$

where V_{ESL} is the volume of solution present during the ESL procedure and V_{PSE} is the volume of solution assessed by the PSE method. C_{ESL} and C_{PSE} are the measured concentrations after ESL or PSE methods, respectively. V_{ESL} and V_{PSE} in Eq. 1 are conventionally calculated as:

$$V_{ESL} = (m_{w,added} + m_{sample} \cdot \%m_{w,evap.}/100)/\rho_w \quad (2)$$

$$V_{PSE} = (m_{sample} \cdot \%m_{w,evap.}/100))/\rho_w \quad (3)$$

where $m_{w,added}$ is the mass of water added for the leaching procedure (g), m_{sample} is the mass of the sample used in the leaching procedure (g), ρ_w is the density of water (g/cm^3), and $\%m_{w,evap.}$ is the evaporable water percentage of the sample measured by drying at 105°C.

Equation 2 representing V_{ESL} is a straightforward calculation of the liquid present during ESL[a]. However, the evaporable water of the ESL powder sample may not accurately represent V_{PSE} in Eq. 3 for the following reasons:

1. Drying may occur during the pulverizing procedure for ESL, which would lead to an underestimation of solution assessed in the PSE procedure. This was shown by Plusquellec et al. to increase the concentration determined by ESL methods [11]. However, the bulk sample drying approach (without pulverizing) still resulted in an overestimated concentration compared to PSE; therefore, sample drying may not be the only source of error when determining V_{PSE} [a].
2. During drying at 105°C, water from phases like ettringite and monosulfate is evaporated. However, X-ray diffraction experiments suggest that the water from these phases is not expressed during PSE [27]. Therefore, evaporable water from hydrated phases could be a source of inaccuracy in correcting ESL results to obtain results similar to PSE.
3. Several studies have shown that the alkali concentrations obtained from PSE are independent of the amount of pressure applied [14,15]. This suggests that the concentration of alkalis exists in equilibrium with the water in the system [14]. Furthermore, calculations of the internal pore pressure during PSE and the measured bound water before and after PSE suggest that interlayer water of C-S-H may be expressed during PSE [27]. Based on these observations, it may be appropriate to consider the entire volume of unreacted pore solution (i.e., not part of a phase) as the volume assessed by PSE (V_{PSE}). Although not all the solution is expressed during PSE, the corrected concentrations from ESL would then be representative of the pore fluid.

Considering these challenges to determining V_{PSE} experimentally – without actually performing PSE and complimentary tests – a theoretical approach to determining V_{PSE} could be more appropriate for the correction of ESL results. This paper presents a method for determining V_{PSE} using the aqueous volume obtained from thermodynamic modeling. We hypothesize that correcting alkali concentrations from ESL using the approach proposed herein for calculating V_{PSE} can reconcile ESL concentrations with those from PSE. The CWE procedure described by Plusquellec et al. [23] was selected based on its suitability for cementitious materials at earlier ages of hydration and extensive literature that informed its development [16–19,21,22,28]. In this paper, both PSE and CWE methods of pore solution extraction were used for three cementitious systems with a range of alkali contents. The focus in this paper is placed on the Na^+ and K^+ concentrations; however, the proposed approach has the potential to be extended to other ions in the pore solution. Different curing temperatures and durations were used to achieve varying degrees of hydration. Solely computational methods for estimating the pore solution composition were also used for comparison.

2 Proposed Approach, CWE_PPM

The proposed methodology of this study builds on experimental data from the existing CWE procedure as an ESL method by utilizing recently developed computation methods that require only input that is commonly available. Figure 1 displays a flowchart of the experimental and computational steps in the proposed approach. The remainder of this section will focus on the computation steps used to determine the theoretical volume of pore solution, $v_{PSE,}$ since this framework is the primary contribution of this study.

[a] In prior studies, $V_{w,ESL}$ and $V_{w,PSE}$ have been calculated following equations 2 and 3 with the same free water measurement used for both. This assumes the amount free water in the ESL and PSE samples are the same. However, ESL would be best represented by the powder sample in actuality, and PSE would theoretically be better represented by bulk sample drying since these reflect the sample preparation used prior to each test.

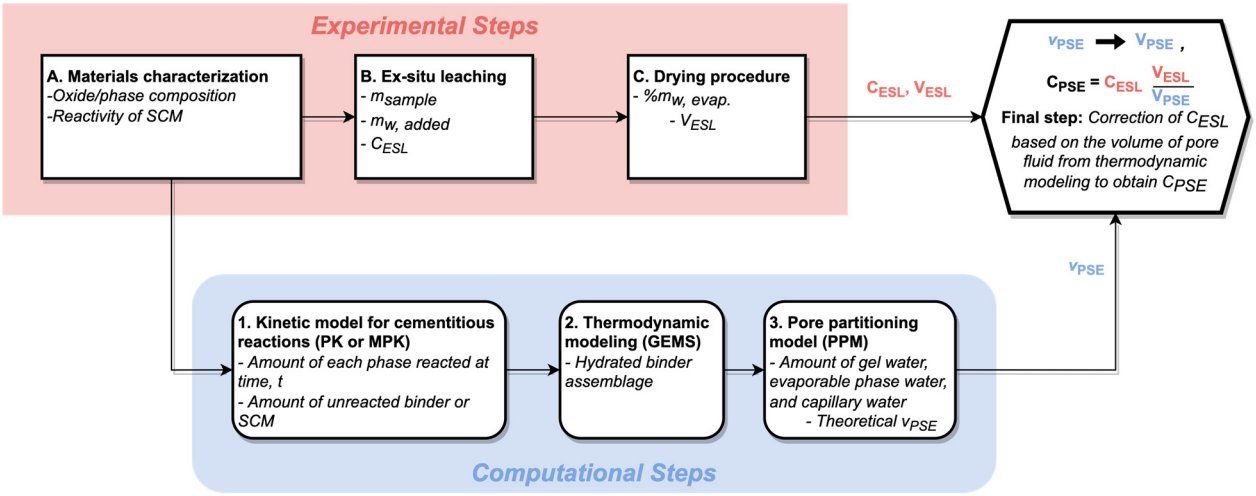

Figure 1. Flowchart of proposed approach for determining the pore solution concentrations of Na^+ and K^+ from ex-situ leaching and thermodynamic modeling.

2.1 Kinetic model of hydration (Step 1)

Using the raw material characterization from step A of Fig. 1, the kinetics of the OPC clinker reactions were simulated using the Parrott and Killoh (PK) model for the OPC mixtures [29], and the modified Parrott and Killoh (MPK) model for OPC + FA mixtures [30]. The reactivity of the fly ash used in this study, which is an indicator for the reactive portion of the material, was determined by the Pozzolanic Reactivity Test [31-34]. Alternatively, the cementitious materials could be analyzed using quantitative X-ray diffraction (QXRD) – from which the crystalline phases and amorphous content of the SCM can be determined. In this approach amorphous content could be used as the reactive portion of the fly ash, as demonstrated by Glosser et al. [35,36]. The PK/MPK model provides the amount each phase that is reacted at time, t, which is the age of samples when ESL tests are performed.

2.2 Thermodynamic modeling (Step 2)

Using only the reactive portion of each phase from the kinetic model, thermodynamic modeling was performed. In this work, we used GEMS3K [37] software coupled with the CEMDATA v18 database [38]. GEMS3K performs thermodynamic modeling by determining the phase assemblage of a cementitious system that minimizes its Gibbs free energy. The GEMS/CEMDATA framework can be used to calculate the molar amounts of solid, aqueous, and gaseous products of reactions and the activities of ions in the pore solutions at thermodynamic equilibrium. The CSHQ model in the CEMDATA databases was used for the mixtures studied in this paper. It is noted that fly ash used in this study has a high Al content, which could lead to the formation of other C-(N,K)-A-S-H phases if the calcium hydroxide in the system is depleted. However, this was not the case for this study, therefore, the CSHQ model was appropriate. Unlikely phases for the samples of this study (e.g., hydrotalcite) were blocked from forming. The assumptions for which C-S-H model is appropriate and which phases should be prohibited from forming should be evaluated on a case-by-case basis for other cementitious systems, particularly if different SCMs are being used. The output of thermodynamic modeling provides the compositional input (e.g., the quantities of the phases such as C-S-H, ettringite, monosulfate, hydrotalcite, and hydrogarnet) used in equations 5-10 of the pore partitioning model (PPM) described in the following section.

2.3 Pore portioning model to determine v_{PSE} (Step 3)

In recent work, thermodynamic calculations have been coupled with a pore partitioning model to account for the total aqueous content as well as the volume of solution that are in the 'classic' capillary and gel pores [39,40]. In this approach, the gel water is assumed to comprise two parts: the water that is released by phases upon heating to 100°C (e.g., ettringite, monosulfate, hydrotalcite, and hydrogarnet) and the portion of water on the surface of phases and in small pores, denoted by β. The calculation of gel water in the PPM is described in detail by Glosser et al. [39] and summarized here for completeness. The process starts with the calculation of released water from the major phases using [40]:

$$v_{w,\ rel.} = \sum_{i=1}^{n,ph} \frac{n_i H_{i,ph} V_{H_2O}}{V_{t,init}} \quad (4)$$

where $v_{w,rel.}$ is the normalized released water volume fraction from all phases (m^3/m^3); i is the index corresponding to a particular phase, n,ph is the number of phases; n_i is the moles of the respective phase, $H_{i,ph}$ is the number of water molecules in each phase; and V_{H_2O} is the molar volume of water (18.015×10^{-6} m^3/mol); and $V_{t,init}$ is the total volume of the initial system (m^3), including water and unhydrated and unreacted material. For $v_{w,rel,}$ the phases which release water here are assumed to be ettringite, monosulfate, and, when present hydrogarnet and hydrotalcite. Equation 4 quantifies the phase water released during drying at 105°C and allows it to be accounted for appropriately in the adjustment of ESL concentrations, which is discussed in section 2.4.

The total volume of gel water in the system is the sum of the phase water (Eq. 4) and the volume of water associated with

the C-S-H. To determine the volume of water associated with the C-S-H, Eq. 5 is used:

$$v_{\mathrm{C-S-H}} = \frac{\sum_{i=1}^{4} n_i (V_{\mathrm{C-S-H}})_i}{v_{t,init}} \quad (5)$$

where $v_{C\text{-}S\text{-}H}$ is the normalized volume of total C-S-H in the system (m^3/m^3), n_i and $(V_{C\text{-}S\text{-}H})_i$ are the number of moles and the molar volume of the C-S-H variant (e.g., jennite, tobermorite, etc.).

Powers and Brownyard proposed that the hydration products can be assumed to have a fixed volume of gel porosity (~26%) for OPC [41]. The normalized volume of gel water can be computed using the Eq. 6a as adapted from Powers and Brownyard by [42]. To apply the Powers-Brownyard (PB) calculations of gel water volumes to thermodynamically modelled systems, a constant, β, is introduced in Eq. 6b,

$$v_{\mathrm{gw,\,PB}} = 0.19(\rho_c/\rho_w)(1-p)\alpha \quad (6a)$$

$$\beta = \frac{v_{\mathrm{gw,PB}} - v_{\mathrm{w,rel.}}}{v_{\mathrm{C-S-H}}} \quad (6b)$$

where $v_{gw,PB}$ is the volume fraction of gel water calculated for OPC from PB equations, ρ_c is the density of cement, p is the initial porosity of the system, and α is the degree of hydration. The coefficient β is determined for an OPC mixture and is then extended to systems including SCMs [39]. For the present study, a constant β of 0.45 was used since this fell in the range of actual values for the OPCs used and typical values for other OPCs (e.g., 0.4 – 0.65 [43]). Using β and the volume of C-S-H calculated by Eq. 5, the volume of gel water associated with C-S-H can be determined as

$$v_{\mathrm{w,\,C-S-H}} = \beta v_{\mathrm{C-S-H}} \quad (7)$$

The volume of C-S-H gel water is used in conjunction with the water released from other hydrated phases calculated by Eq. 4 to compute the total gel water:

$$v_{\mathrm{w,gel}} = v_{\mathrm{w,rel.}} + v_{\mathrm{w,\,C-S-H}} \quad (8)$$

The balance of the water in the system is assumed to be capillary water. The capillary water volume can be calculated as follows:

$$v_{\mathrm{w,cap.}} = v_{\mathrm{aq.}} - \left(v_{\mathrm{w,gel}} - v_{\mathrm{w,rel.}}\right) \quad (9)$$

where $v_{w,cap.}$ is the total capillary water and $v_{aq.}$ is excess unreacted solution from thermodynamic calculations. The theoretical volume fraction of pore solution accounted for by PSE can then be represented by

$$v_{\mathrm{PSE}} = v_{\mathrm{w,cap.}} + v_{\mathrm{w,C-S-H}} \quad (10)$$

Note that v_{PSE} is effectively equal to $v_{aq.}$. However, the distinction of capillary and gel water is necessary for implementing v_{PSE} in the concentration adjustment, which will be described in the following section [30-34,37,38].

2.4 Adapting v_{PSE} to adjust ESL concentrations

Because v_{PSE} is a normalized volume from the PPM, determining the theoretical volume, V_{PSE}, for a specific ESL sample requires scaling the fraction to the ESL sample size. Equation 11 accommodates ESL samples of any moisture content. Using the ESL sample mass and values from thermodynamic modeling V_{PSE} can be calculated as

$$m_{\mathrm{dry\ sample}} = m_{\mathrm{sample}} \cdot \left(1 - \frac{\%m_{\mathrm{w,evap.}}}{100}\right) \quad (11a)$$

$$\rho_{\mathrm{dry}} = \left(\frac{m_{\mathrm{solids}} - m_{\mathrm{w,rel.}}}{v_{\mathrm{solids}} + v_{\mathrm{ub}} - v_{\mathrm{w,rel.}}}\right) \quad (11b)$$

$$\frac{v_t}{v_{\mathrm{dry}}} = \left(\frac{1}{v_{\mathrm{solids}} + v_{\mathrm{ub}} - v_{\mathrm{w,rel.}}}\right) \quad (11c)$$

$$V_{\mathrm{PSE}} = \left(\frac{m_{\mathrm{dry\ sample}}}{\rho_{\mathrm{dry}}}\right) \cdot \left(\frac{v_t}{v_{\mathrm{dry}}}\right) \cdot v_{\mathrm{PSE}} \quad (11d)$$

where $m_{dry\ sample}$ is the experimentally determined dry sample mass (g), ρ_{dry} is the dry density of the system (g/cm^3) and v_t/v_{dry} is the ratio of total volume to the dry volume. Both ρ_{dry} and v_t/v_{dry} were determined from the thermodynamic model output with the use of $v_{w,\,rel.}$ from the PPM to account for phase water lost during sample drying at 105°C. The mass and volume of solids (m_{solids} and v_{solids}) can be obtained directly from thermodynamic model output and the volume of unreacted binder (v_{ub}) is known from the kinetic model.

While determining V_{PSE} using Eq. 3 was potentially influenced by moisture loss during sample preparation, Eq. 11 normalizes the sample moisture content based on the thermodynamic data. This effectively means that ESL samples of any moisture content can be used in the present method, or without the need for a separate bulk drying sample recommended by other authors [11,24].

3 Experimental Study

3.1 Materials

Three paste mixtures were prepared for this study using two different curing temperatures to achieve varying degrees of hydration. A low alkali portland cement (PC), high alkali cement (HA), and a Class F fly ash were used in this study. The oxide compositions are shown in Table 1. Each cement constituted its own mixture (denoted as PC and HA), and the third mixture used the low alkali cement with 25% wt. fly ash replacement (denoted as FA). All mixtures used a w/b of 0.47 by mass. Samples were cast in 50 mm (diameter) x 100 mm (length) plastic cylinders with tight fitting plastic caps, which were then sealed over with foil tape. To prevent bleeding, the cylinders were rotated at 75 rpm for 24 hours after casting. The cylinders were demolded after 24 hours and sealed in air-tight plastic bags and stored at two different temperatures: 23°C and 80°C. The 80°C samples were kept sealed and stored for 15 days over water to prevent help evaporation. The cylinders stored at 23°C were kept sealed for 28 days before testing.

Table 1. Oxide composition of cements and fly ash.

wt. %	Low alkali OPC (PC)	High alkali OPC (HA)	Fly Ash (FA)
SiO_2	20.5	20.5	51.9
Al_2O_3	4.05	5.26	21.7
Fe_2O_3	3.62	2.11	5.04
CaO	61.7	64.2	8.61
MgO	2.52	1.40	2.58
SO_3	1.80	4.28	0.78
Na_2O	0.17	0.15	2.58
K_2O	0.69	1.23	1.45
Na_2O_{eq}	0.62	0.96	3.50
LOI	1.96	-	1.42

3.2 Methods

3.2.1 Pore Solution Extraction (PSE)

The high-pressure extraction of pore solution was performed using the apparatus described in [44] and the method for pastes described in [45]. A maximum pressure of 320 MPa was held constant for 1 minute once attained and then the pressure was released. The pH of solutions was measured at room temperature using a probe immediately after expression. The expressed solutions were stored in syringes to minimize air contact, and the syringes were then stored at 5°C in air-tight plastic bags until being analyzed. The solutions were vacuum filtered through 0.45 µm cellulose filters before being diluted for inductive coupled plasma optical emission spectroscopy (ICP-OES, Spectros Arcos) analysis. The filtered solutions were diluted with 2% nitric acid at dilution factor of 20x for Ca, Al, and Si ions, and 100x for Na, K, and S ions.

3.2.2 Thermogravimetric Analysis

Powder samples prepared for the CWE procedure described in section 3.5 were also analyzed by thermogravimetric analysis (TGA, Q50, TA instruments). The 40-45 mg sample was heated at a rate of 10°C/min up to 1000°C in a 9 mm diameter crucible with a 60 mL/min [46]. flow of nitrogen over the sample. The mass loss at $m_{105°C}$ was taken as the evaporable water content. TGA results for different mixtures under different curing regimes are presented in Table A1 and Figures A1-A3 of the Appendix. TGA is not necessary for the determination of $\%m_{w,\,evap.}$ in the proposed framework, but mass equilibrium at 105°C should be ensured in whatever drying method is used for step C of Fig. 1.

3.2.3 Pozzolanic Reactivity Test

The Pozzolanic Reactivity Test (PRT) was performed to determine the maximum degree of reactivity (DOR*) of the SCM used in this study [31,34]. A 40 g sample of SCM was mixed with 120 g of dry reagent grade calcium hydroxide (CH, SCM to CH ratio of 1:3) and 144 g of 0.5 M KOH (liquid-to-solid ratio of 9:10). Approximately 7 g of sample was then transferred to an isothermal calorimeter (TAMair), which had been preconditioned at 50±2°C for 24 hours. After 45 minutes of signal stabilization, the heat flow of the calorimeter was recorded for 10 days. After 10 days, the sample was removed from the calorimeter and a 20 mg sample was used to determine the remaining CH content from TGA [31,47]. The DOR* for the fly ash used in this study was 37.15% as reported in detail elsewhere [32,33]. The DOR* value was then used in the modified Parrot-Killoh (MPK) [30] to determine the oxide content of the fly ash to include in thermodynamic modelling of the samples in this study.

3.2.4 NIST Pore Solution Calculator

The pore solution composition of samples was estimated using the NIST pore solution calculator [48]. The method is based on prior work suggesting that roughly 75% of alkalis can be assumed to be free in the pore solution after sulfate is depleted [49]. The alkali contents from Table 1 were used as input for each mixture. The DoH of each respective sample determined from TGA as $(m_{140°C} - m_{1000°C})/0.23$, following [46], was also used as input.

3.2.5 Cold-Water Extraction (CWE)

Samples for CWE were first ground to pass a 75-micron sieve using a combination of a steel-tipped hammering device [15], and a steel mortar and pestle with the total sample exposure time to air limited to ~15 min to minimize carbonation. CWE samples were stored in air-tight bags between grinding and testing. The 5-minute leaching procedure with vacuum filtration over Whatman filter paper as described by [11] was followed for three replicates of each sample. The solution was then placed in cups assembled with a polypropylene film base and analyzed using the XRF to determine the Na^+, K^+, SO_4^{2+}, Al^{3+}, and Ca^{2+} concentrations – a method shown to yield comparable results to ICP-OES [50,51]. Concentrations (mmol/L) were calculated from the mass abundance (g/1000L) using the molar mass of each element.

The adjustment of CWE concentrations was made using the free water content determined from 105°C drying with Eq. 3 and these results are denoted as CWE_105°C. The CWE results were also corrected in the newly proposed approach incorporating PPM results with Eq. 11 and these results are distinguished as CWE_PPM.

4 Results and Discussion

4.1 Comparison of ESL Correction Approaches

The PPM results for the six samples of this study are shown in Fig. 2. The aqueous contents in the PPM rely on thermodynamic data from each specific system, and differences between the samples are represented in Fig. 2. Samples cured at 80°C for 15 days exhibited a greater amount of gel solids and lower overall water content. The mixture containing fly ash had the highest unreacted binder content according to PPM, which can be expected for the age of samples tested ($\leq$ 28 days). As discussed earlier, using aqueous volumes from PPM in Eq. 11 may address the potential issues with using Eq. 3 and the evaporable water content for adjusting ESL concentrations.

Figure 3 shows a comparison of concentrations obtained from CWE with corrections using Eq. 3 (CWE_105°C), the proposed approach for CWE correction using PPM (CWE_PPM, $v_{\mathrm{w,PSE}} = v_{\mathrm{w,cap.}} + v_{\mathrm{w,C-S-H}}$), and several scenarios of what the results would be if Eq. 10 were altered (*) so V_{PSE} would be comprised of only capillary water ($*\,v_{\mathrm{w,PSE}} = v_{\mathrm{w,cap.}}$) or capillary and released phase water ($*\,v_{\mathrm{w,PSE}} = v_{\mathrm{w,cap.}} + v_{\mathrm{w,rel.}}$) from the PPM results.

The water contents from PPM and drying used to calculate the results shown in Fig. 3 are reported in Table A1. The combined [$Na^+ + K^+$] is used in this section since the same CWE measurements are being evaluated with different concentrations adjustments for the added water during ESL and the ratio of the ions does not change [14]. Separate Na^+ and K^+ concentrations are shown in section 4.2. The PSE results shown here were discussed in greater detail elsewhere with respect to the effect of sample type on alkalinity [52].

As seen in Fig. 3, including only capillary water from PPM in the correction does not fully account for the difference between ESL and PSE results. Including capillary and released phase water in the correction improves the correlation to PSE, but only for samples cured at 23°C. This is because samples cured at 80°C did not include ettringite or monosulfate as released phases since their formation is destabilized at elevated temperatures [53]. The CWE_105C samples cured at 23°C are also closer to the PSE than samples cured at 80°C because the released phase water is included in the 105°C drying process. The CWE_PPM results are consistently closer to a 1:1 relationship with PSE results than CWE_105C, regardless of curing temperature. This supports our hypothesis that Eq. 10 is a more accurate representation of V_{PSE} than Eq. 3.

Fig. 4a compares the concentrations obtained from CWE (CWE_105°C) and the proposed approach (CWE_PPM) to that of PSE with the variability of the methods indicated with error bars. The error bars in Fig. 4a suggest that there is low variability between trials in the CWE method with either approach for adjusting concentrations. While there is low variability in the CWE method itself, the free water determination can have a strong influence on results according to studies using Eq. 3 when adjusting concentrations [11,24].

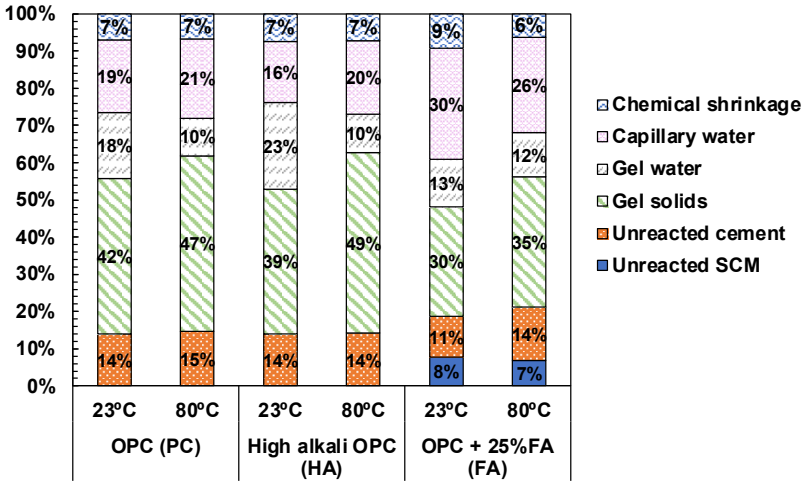

Figure 2. Pore partitioning model results showing unreacted binder, gel solids, gel water, capillary water, and chemical shrinkage volume percentages.

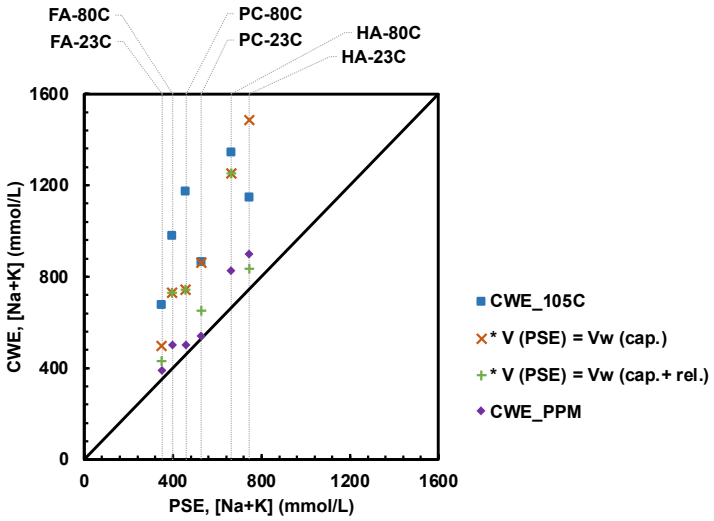

Figure 3. Comparison of total alkali concentrations from PSE to CWE using various approaches for adjusting concentrations. Vertical lines and labels identify samples. Cases marked with an asterisk (*) are alternatives to Eq. 10 (used to calculate CWE_PPM) and are only included for discussion purposes.

Fig. 4b shows the results of a sensitivity analysis of the CWE results indicating how hypothetical changes (+/- 5%) of $m_{w, evap.}$ affect the alkali content predictions. The results of CWE_105C are strongly affected by this change, and this is consistent with the observations of other studies [11,24]. However, the CWE_PPM results see minimal effect since Eq. 11 was used to calculate V_{PSE} and $\%m_{w, evap.}$ only makes up a small portion of V_{CWE} compared to $V_{w,added}$ in Eq. 2. The proposed adjustment method of CWE_PPM effectively mitigates the dependency of results on the free water determination. The variability between trials and sensitivity analysis shown in Fig. 4 demonstrate that the difference between CWE_105C and CWE_PPM is substantial and unlikely to be attributed to experimental error.

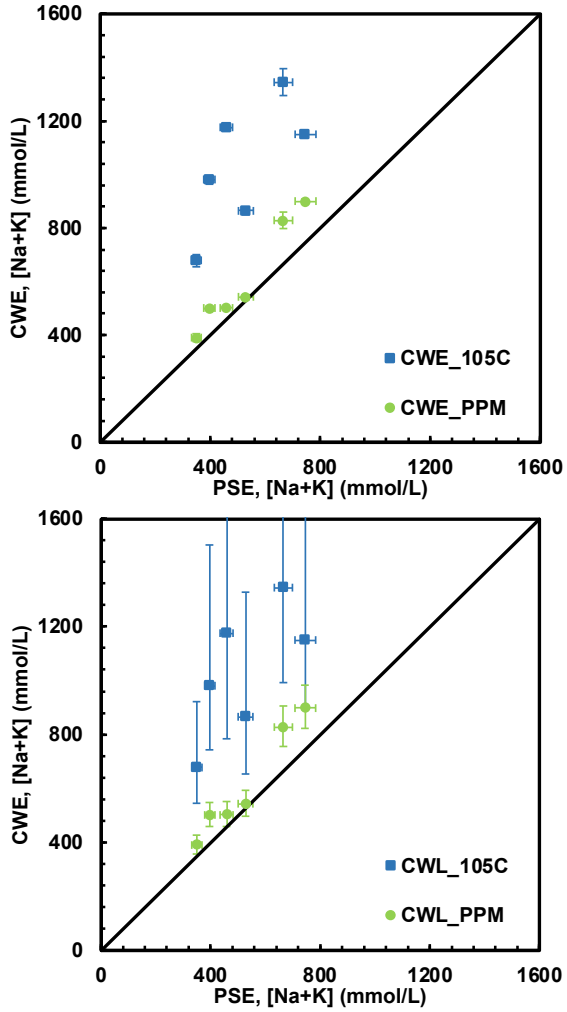

Figure 4. Comparison of CWE_105C and CWE_PPM to PSE. Vertical error bars either represent plus or minus one standard deviation between CWE repeat trials (top) or the hypothetical effect of increasing or decreasing $\%m_{w, evap.}$ by 5% in the CWE adjustment (bottom). For horizontal error bars assigned to PSE, 5% error was assumed based on the data presented in [15].

Considering the variability between trials and the impact of sample moisture content are low for CWE_PPM results, the remaining sources of error – i.e. causes for discrepancy between CWE_PPM and PSE – are limited. The sampling difference between PSE and CWE are one possible source of error, since mixtures and cast samples may not have been completely homogenous. Approximations made during thermodynamic modeling and pore partitioning may have also resulted in slight discrepancies between the aqueous contents of the PPM and the actual samples. These sources of error are relatively small for the paste samples of this study since there is a good overall agreement between CWE_PPM and PSE in terms of alkali concentrations (Fig. 4), but they may be more significant when scaling the method to mortars or concrete.

4.2 Comparing Different Methods for Pore Solution Determination

In addition to CWE and PSE experimental results, the pore solution alkali content was also modeled using thermodynamic calculations (GEMS) and the NIST calculator. Fig. 5 shows the correlation of these modeling approaches and CWE_PPM to PSE. Here, Na^+ and K^+ concentrations are shown separately since they are considered differently in thermodynamic modeling.

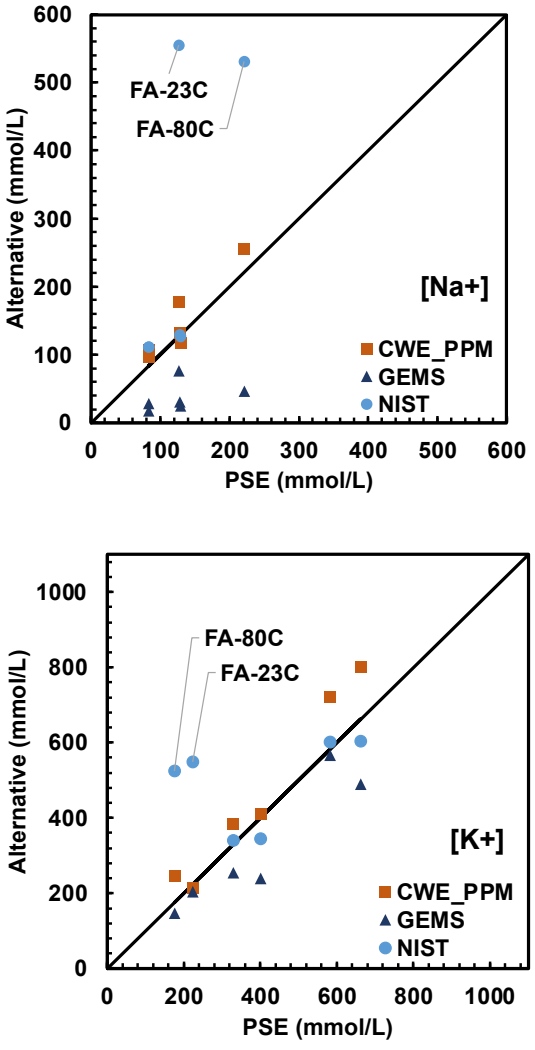

Figure 5. Comparison of alternatives to PSE for a) [Na^+], and b) [K^+]. CWE results had less than 5% coefficient of variation between trials on average.

The results from CWE_PPM show a similar correlation to PSE in Fig. 5, regardless of ion type. However, GEMS results appear to be more accurate for K^+ than Na^+. This could be attributed to several aspects in the modeling approach of GEMS that ultimately assigns bound alkalis as C-S-H end members to represent their exclusion from the pore solution. While the CSHQ model of C-S-H was used in GEMS for the present study [37], future work implementing the recently developed CASH+ model of C-S-H end members with extensions for alkali incorporation [54,55] could help improve alkali concentrations from GEMS with respect to concentrations from PSE.

The NIST results were less sensitive to ion type and have two outliers for the fly ash mixture as shown in Fig. 5. The NIST model does not consider fly ash as potential source of increased alkali binding or sulfate, and only considers the fly ash as an additional source of alkalis. However, the additional C-S-H formation from fly ash in the mixture likely increases the amount of bound alkali. Shehata and Thomas showed that mixtures containing fly ash had lower alkali releases than the OPC control and a mixture containing only silica fume [56]. While predictive methods (NIST and GEMS) make certain assumptions to estimate the alkali content of the pore solution, our proposed approach, CWE_PPM, incorporates experimental ESL measurements to yield a consistent relationship with PSE.

5 Conclusions

When using ex-situ leaching methods, such as CWE, the accuracy of results relies on both the leaching procedure to determine a diluted concentration of ions and the determination of the volumes of solution used for adjusting the diluted concentrations to reflect PSE concentrations. The proposed computational approach for adjusting of CWE concentrations, CWE_PPM, was shown to have several advantages over the conventional free water correction based on drying at 105°C, CWE_105C:

1. The results of CWE_PPM were essentially independent of the measured moisture content of the sample – eliminating drying during sample preparation as a major source of error. In the context of implementing ESL for examining field structures, this implies that a relatively small powder sample could be obtained for complete ESL analysis.
2. Thermodynamic modeling allowed evaporable phase water from phases like ettringite and monosulfate to be excluded from V_{PSE}.
3. In conjunction with the first two advantages of CWE_PPM over CWE_105C, using thermodynamic modeling to determine aqueous content for V_{PSE} led to an improved correlation to PSE.

Further research is needed to demonstrate that the proposed method for adjusting ESL concentrations can be scaled for use with concrete samples and thermodynamic models of a wider range of cementitious systems. The CWE_PPM method in this paper is a promising alternative to PSE and is appears to be more reliable and scalable than purely predictive methods.

Acknowledgments

AT's involvement was funded by the National Science Foundation under Grant #EEC-2127509 administrated by the American Society for Engineering Education. The participation of other authors and experimental resources were not externally funded.

Authorship statement (CRediT)

Atolo Tuinukuafe: Conceptualization, Methodology, Formal analysis, Investigation, Writing - Original Draft, Visualization, Funding acquisition

Krishna Siva Teja Chopperla: Investigation, Formal analysis, Writing - Review & Editing

W. Jason Weiss: Methodology, Resources, Writing - Review & Editing

Jason H. Ideker: Supervision, Resources, Writing - Review & Editing, Funding acquisition

O. Burkan Isgor: Conceptualization, Methodology, Formal analysis, Writing – Original Draft, Supervision, Funding acquisition

Appendix

Table A1. Water contents from drying (TGA) and PPM.

Sample		Mass fraction of water from drying	Volume fraction of water from PPM		
		105°C	cap.	rel.	C-S-H
OPC (PC)	23°C	12%	19%	6%	11%
	80°C	8%	23%	0%	9%
High alkali OPC (HA)	23°C	13%	16%	13%	11%
	80°C	11%	20%	0%	12%
OPC + 25%FA (FA)	23°C	15%	30%	4%	8%
	80°C	12%	26%	0%	12%

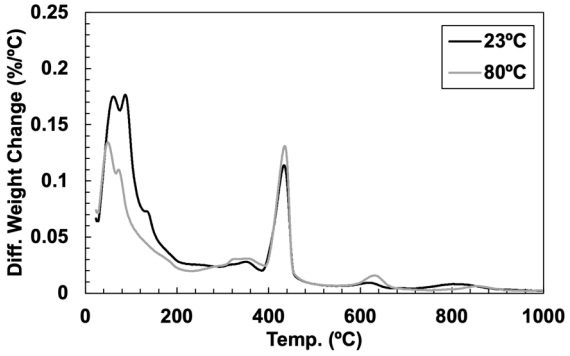

Figure A1. TGA results for PC mixture with different curing regimes.

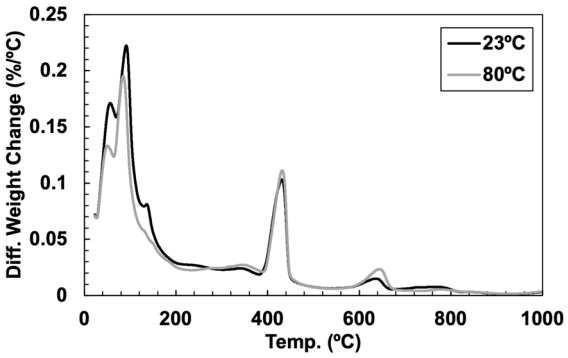

Figure A2. TGA results for HA mixture with different curing regimes.

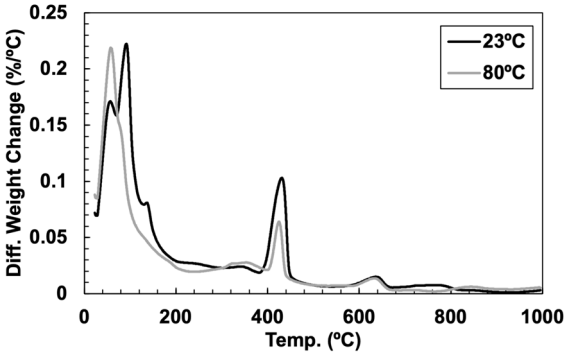

Figure A3. TGA results for FA mixture with different curing regimes.

6 References

[1] P. Ghods, O.B. Isgor, G.J.C. Carpenter, J. Li, G.A. McRae, G.P. Gu, Nano-scale study of passive films and chloride-induced depassivation of carbon steel rebar in simulated concrete pore solutions using FIB/TEM, Cem Concr Res. 47 (2013) 55-68. https://doi.org/10.1016/j.cemconres.2013.01.009

[2] K.A. Snyder, X. Feng, B.D. Keen, T.O. Mason, Estimating the electrical conductivity of cement paste pore solutions from OH-, K+ and Na+ concentrations, Cem Concr Res. 33 (2003) 793-798. https://doi.org/10.1016/S0008-8846(02)01068-2

[3] U.M. Angst, M.R. Geiker, M.C. Alonso, R. Polder, O.B. Isgor, B. Elsener, H. Wong, A. Michel, K. Hornbostel, C. Gehlen, R. François, M. Sanchez, M. Criado, H. Sørensen, C. Hansson, R. Pillai, S. Mundra, J. Gulikers, M. Raupach, J. Pacheco, A. Sagüés, The effect of the steel-concrete interface on chloride-induced corrosion initiation in concrete: a critical review by RILEM TC 262-SCI, Materials and Structures 52 (2019). https://doi.org/10.1617/s11527-019-1387-0

[4] J. Williamson, O.B. Isgor, The effect of simulated concrete pore solution composition and chlorides on the electronic properties of passive films on carbon steel rebar, Corros Sci. 106 (2016) 82-95. https://doi.org/10.1016/j.corsci.2016.01.027

[5] R. Spragg, C. Qiao, T. Barrett, J. Weiss, Assessing a concrete's resistance to chloride ion ingress using the formation factor, in: Corrosion of Steel in Concrete Structures, Elsevier Inc., 2016: 211-238. https://doi.org/10.1016/B978-1-78242-381-2.00011-0

[6] V. Jafari Azad, A.R. Erbektas, C. Qiao, O.B. Isgor, W.J. Weiss, Relating the Formation Factor and Chloride Binding Parameters to the Apparent Chloride Diffusion Coefficient of Concrete, Journal of Materials in Civil Engineering. 31 (2019) 04018392. https://doi.org/10.1061/(ASCE)MT.1943-5533.0002615

[7] J.H. Ideker, B.L. East, K.J. Folliard, M.D.A. Thomas, B. Fournier, The current state of the accelerated concrete prism test, Cem Concr Res. 40 (2010) 550-555. https://doi.org/10.1016/j.cemconres.2009.08.030

[8] F. Rajabipour, E. Giannini, C. Dunant, J.H. Ideker, M.D.A. Thomas, Alkali-silica reaction: Current understanding of the reaction mechanisms and the knowledge gaps, Cem Concr Res. 76 (2015) 130-146. https://doi.org/10.1016/j.cemconres.2015.05.024

[9] G. Plusquellec, M.R. Geiker, J. Lindgård, K. de Weerdt, Determining the free alkali metal content in concrete - Case study of an ASR-affected dam, Cem Concr Res. 105 (2018) 111-125. https://doi.org/10.1016/j.cemconres.2018.01.003

[10] S. Manso, A. Aguado, A review of sample preparation and its influence on pH determination in concrete samples, Materiales de Construccion. 67 (2017). https://doi.org/10.3989/mc.2017.08515

[11] G. Plusquellec, M.R. Geiker, J. Lindgård, J. Duchesne, B. Fournier, K. de Weerdt, Determination of the pH and the free alkali metal content in the pore solution of concrete: Review and experimental comparison, Cem Concr Res. 96 (2017) 13-26. https://doi.org/10.1016/j.cemconres.2017.03.002

[12] R.S. Barneyback, S. Diamond, Expression and analysis of pore fluids from hardened cement pastes and mortars, Cem Concr Res. 11 (1981) 279-285. https://doi.org/10.1016/0008-8846(81)90069-7

[13] M.-A. Bérubé, C. Tremblay, Chemistry of pore solution expressed under high pressure-influence of various parameters and comparison with the hot-water extraction method, in: Proceedings of the 12th International Conference on Alkali-Aggregate Reaction in Concrete, 2004: 833-842.

[14] J. Duchesne, M.A. Berube, Evaluation of the validity of the pore solution expression method from hardened cement pastes and mortars, Cem Concr Res. 24 (1994) 456-462. https://doi.org/10.1016/0008-8846(94)90132-5

[15] L. Montanari, J. Tanesi, H. Kim, A. Ardani, Influence of loading pressure and sample preparation on ionic concentration and resistivity of pore solution expressed from concrete samples, J Test Eval. 49 (2020). https://doi.org/10.1520/JTE20190765

[16] V. Räsänen, V. Penttala, The pH measurement of concrete and smoothing mortar using a concrete powder suspension, Cem Concr Res. 34 (2004) 813-820. https://doi.org/10.1016/j.cemconres.2003.09.017

[17] P.Y. Loh, P. Shafigh, H.Y.B. Katman, Z. Ibrahim, S. Yousuf, Ph measurement of cement-based materials: The effect of particle size, Applied Sciences (Switzerland). 11 (2021). https://doi.org/10.3390/app11178000

[18] L. Li, J. Nam, W.H. Hartt, Ex situ leaching measurement of concrete alkalinity, Cem Concr Res. 35 (2005) 277-283. https://doi.org/10.1016/j.cemconres.2004.04.024

[19] W.C. Wang, W.H. Huang, M.Y. Lee, H.T.H. Duong, Y.H. Chang, Standardized procedure of measuring the ph value of cement matrix material by ex-situ leaching method (Esl), Crystals (Basel). 11 (2021). https://doi.org/10.3390/cryst11040436

[20] V. Pavlik, Water extraction of chloride, hydroxide and other ions from hardened cement pastes, Cem Concr Res. 30 (2000) 895-906. https://doi.org/10.1016/S0008-8846(00)00261-1

[21] M.C. Alonso, J.L. García Calvo, A. Hidalgo, L. Fernández Luco, Development and application of low-pH concretes for structural purposes in geological repository systems, in: Geological Repository Systems for Safe Disposal of Spent Nuclear Fuels and Radioactive Waste, Elsevier Inc., 2010: 286-322. https://doi.org/10.1533/9781845699789.3.286

[22] M.C. Castellote, M.C. Alonso, C. Andrade, Determinación del contenido de OH- en la fase acuosa de los poros de matrices cementantes por un método empírico de lixiviación, Materiales de Construcción. 52 (2002). https://doi.org/10.3989/mc.2002.v52.i265.343

[23] G. Plusquellec, N. Klaartje, D. Weerdt, Cold water extraction (CWE) Procedure for the determination of the alkali content and pore solution composition, http://www.ivt.ntnu.no/kt/

[24] K. Natkunarajah, K. Masilamani, S. Maheswaran, B. Lothenbach, D.A.S. Amarasinghe, D. Attygalle, Analysis of the trend of pH changes of concrete pore solution during the hydration by various analytical methods, Cem Concr Res. 156 (2022) 106780. https://doi.org/10.1016/j.cemconres.2022.106780

[25] M. Berube, J. Frenette, M. Rivest, D. Vezina, Measurement of the Alkali Content of Concrete Using Hot-Water Extraction, Cement, Concrete, and Aggregates. 24 (2002) 28-36. https://doi.org/10.1520/CCA10489J

[26] B. Fournier, L. Sanchez, J. Duchesne, S. Goyette, Evaluation of the Available Alkali Content in Concrete Through a Modified Hot-Water Extraction Method, 15th International Conference on Alkali Aggregate Reaction. (2016).

[27] J. Xu, K. Zheng, L. Chen, X. Zhou, Q. Yuan, Effect of Pore water expression on solid composition of cement paste, Advances in Cement Research. (2021). https://doi.org/10.1680/jadcr.21.00122

[28] M.C. Alonso, J.L. Calvo García, C. Walker, M. Naito, S. Pettersson, I. Puigdomenech, M.A. Cuñado, M. Vuorio, Posiva, H. Ueda, K. Fujisaki, Development of an accurate pH measurement methodology for the pore fluids of low pH cementitious materials, 2012. www.skb.se.
[29] L.J. Parrott, D.C. Killoh, Prediction of cement hydration, Proceedings of the British Ceramic Society. 35 (1984) 41-53.
[30] D. Glosser, P. Suraneni, O.B. Isgor, W.J. Weiss, Estimating reaction kinetics of cementitious pastes containing fly ash, Cem Concr Compos. 112 (2020). https://doi.org/10.1016/j.cemconcomp.2020.103655
[31] D. Glosser, A. Choudhary, O.B. Isgor, W.J. Weiss, Investigation of reactivity of fly ash and its effect on mixture properties, ACI Mater J. 116 (2019) 193-200. https://doi.org/10.14359/51716722
[32] K. Bharadwaj, K.S.T. Chopperla, A. Choudhary, D. Glosser, R.M. Ghantous, G. Vasudevan, J.H. Ideker, B. Isgor, D. Trejo, W.J. Weiss, CALTRANS: Impact of the Use of Portland-Limestone Cement on Concrete Performance as Plain or Reinforced Material Final Report, 2022. https://doi.org/10.5399/osu/1150
[33] K. Bharadwaj, O. Burkan Isgor, W.J. Weiss, A Dataset Containing Statistical Compositions and Reactivities of Commercial and Novel Supplementary Cementitious Materials Dataset Version 1.0, (2022). https://doi.org/10.5399/osu/1152.
[34] K. Bharadwaj, O.B. Isgor, W.J. Weiss, A Simplified Approach to Determine Pozzolanic Reactivity of Commercial Supplementary Cementitious Materials, Concrete International. (2022) 27-32.
[35] D. Glosser, O.B. Isgor, W.J. Weiss, Non-equilibrium thermodynamic modeling framework for ordinary portland cement/supplementary cementitious material systems, ACI Mater J. 117 (2020) 111-123. https://doi.org/10.14359/51728127
[36] D. Glosser, P. Suraneni, O.B. Isgor, W.J. Weiss, Using glass content to determine the reactivity of fly ash for thermodynamic calculations, Cem Concr Compos. 115 (2021). https://doi.org/10.1016/j.cemconcomp.2020.103849
[37] D.A. Kulik, Improving the structural consistency of C-S-H solid solution thermodynamic models, Cem Concr Res. 41 (2011) 477-495. https://doi.org/10.1016/j.cemconres.2011.01.012
[38] B. Lothenbach, D.A. Kulik, T. Matschei, M. Balonis, L. Baquerizo, B. Dilnesa, G.D. Miron, R.J. Myers, Cemdata18: A chemical thermodynamic database for hydrated Portland cements and alkali-activated materials, Cem Concr Res. 115 (2019) 472-506. https://doi.org/10.1016/j.cemconres.2018.04.018
[39] D. Glosser, V.J. Azad, P. Suraneni, O.B. Isgor, W.J. Weiss, Extension of powers-Brownyard model to pastes containing supplementary cementitious materials, ACI Mater J. 116 (2019) 205-216. https://doi.org/10.14359/51714466
[40] V.J. Azad, P. Suraneni, O.B. Isgor, W.J. Weiss, Interpreting the pore structure of hydrating cement phases through a synergistic use of the powers-Brownyard model, hydration kinetics, and thermodynamic calculations, Adv Civ Eng Mater. 6 (2017) 1-16. https://doi.org/10.1520/ACEM20160038
[41] T.C. Powers, T.L. Brownyard, Studies of the Physical Properties of Hardened Portland Cement Paste, Portland Cement Association Bulletin. 22 (1948).
[42] O.M. Jensen, P.F. Hansen, Water-entrained cement-based materials I. Principles and theoretical background, Cem Concr Res. 31 (2001) 647-654. https://doi.org/10.1016/S0008-8846(01)00463-X
[43] Keshav Bharadwaj, Towards the Development of Performance-Based Concrete Mixtures Made with Modern Cementitious Materials Using Thermodynamic Modeling, PhD Dissertation, Oregon State University, 2022.
[44] M.P. Adams, Factors Influencing Conversion and Volume Stability in Calcium Aluminate Cement Systems, 2015.
[45] K.S.T. Chopperla, T. Drimalas, M. Beyene, J. Tanesi, K. Folliard, A. Ardani, J.H. Ideker, Combining reliable performance testing and binder properties to determine preventive measures for alkali-silica reaction, Cem Concr Res. 151 (2022). https://doi.org/10.1016/j.cemconres.2021.106641
[46] I. Pane, W. Hansen, Investigation of blended cement hydration by isothermal calorimetry and thermal analysis, Cem Concr Res. 35 (2005) 1155-1164. https://doi.org/10.1016/j.cemconres.2004.10.027
[47] T. Kim, J. Olek, Effects of sample preparation and interpretation of thermogravimetric curves on calcium hydroxide in hydrated pastes and mortars, Transp Res Rec. (2012) 10-18. https://doi.org/10.3141/2290-02
[48] D.P. Bentz, A virtual rapid chloride permeability test, Cem Concr Compos. 29 (2007) 723-731. https://doi.org/10.1016/j.cemconcomp.2007.06.006
[49] H.F.W. Taylor, A method for predicting alkali ion concentrations in cement pore solutions, Advances in Cement Research. 1 (1987). https://doi.org/10.1680/adcr.1987.1.1.5
[50] M.T. Chang, P. Suraneni, O.B. Isgor, D. Trejo, W.J. Weiss, Using X-ray fluorescence to assess the chemical composition and resistivity of simulated cementitious pore solutions, Int J Adv Eng Sci Appl Math. (2017). https://doi.org/10.3109/01676830.2015.1078376
[51] M. Tsui-Chang, P. Suraneni, J.F. Muñoz, W.J. Weiss, L. Montanari, Determination of Chemical Composition and Electrical Resistivity of Expressed Cementitious Pore Solutions Using X-Ray Fluorescence, ACI Mater J. 116 (2018) 155-164. https://doi.org/10.14359/51712242
[52] K.S.T. Chopperla, J.H. Ideker, A study on the effect of aggregate type on pore solution composition, in: A.L., Batista, S.S., Silva, I., Fernandes, L.O., Santos, J. Custódio, Serra (Eds.), 16th International Conference on Alkali Aggregate Reaction in Concrete, Laboratório Nacional de Engenharia Civil, Lisbon, Portugal, 2022: 501-511.
[53] F. Deschner, B. Lothenbach, F. Winnefeld, J. Neubauer, Effect of temperature on the hydration of Portland cement blended with siliceous fly ash, Cem Concr Res. 52 (2013) 169-181. https://doi.org/10.1016/j.cemconres.2013.07.006
[54] D.A. Kulik, G.D. Miron, B. Lothenbach, A structurally-consistent CASH+ sublattice solid solution model for fully hydrated C-S-H phases: Thermodynamic basis, methods, and Ca-Si-H2O core sub-model, Cem Concr Res. 151 (2022). https://doi.org/10.1016/j.cemconres.2021.106585
[55] G.D. Miron, D.A. Kulik, Y. Yan, J. Tits, B. Lothenbach, Extensions of CASH+ thermodynamic solid solution model for the uptake of alkali metals and alkaline earth metals in C-S-H, Cem Concr Res. 152 (2022). https://doi.org/10.1016/j.cemconres.2021.106667
[56] M.H. Shehata, M.D.A. Thomas, Alkali release characteristics of blended cements, Cem Concr Res. 36 (2006) 1166-1175. https://doi.org/10.1016/j.cemconres.2006.02.015